

# Effects of Symmetry Breakdown in the Bifurcations of Periodic Orbits of a Non-integrable Hamiltonian System

S. D. PRADO AND M. A. M. DE AGUIAR

*Instituto de Física “Gleb Wataghin,” UNICAMP, 13081-970 Campinas-SP, Brazil*

Received January 22, 1993; revised June 14, 1993

In this work we study numerically the breakdown of discrete symmetries in a Hamiltonian system with two degrees of freedom. The initial Hamiltonian is invariant under time-reversal ( $t \rightarrow -t$ ) and reflexion through an axis ( $x \rightarrow -x$ ). These symmetries are then broken by the insertion of a magnetic field and a term of the form  $\gamma x^3$ . The effects of these perturbations are studied in terms of Poincaré sections and periodic orbits. © 1994 Academic Press, Inc.

## I. INTRODUCTION

Physical systems that remain invariant under certain transformations are very common. These symmetries, however, are frequently broken by generic perturbations produced by interactions with other systems or by external noises. An important example is the class of systems invariant under time-reversal. In this case, the introduction of magnetic fields breaks this symmetry if the system has electric changes.

In this work we consider a non-integrable Hamiltonian system with two degrees of freedom that has, initially, two discrete symmetries: time-reversal ( $t \rightarrow -t$ ) and reflexion through an axis ( $x \rightarrow -x$ ). The presence of such symmetries gives rise to qualitatively different structures in the phase-space. One particularly important feature is the change of the bifurcation patterns undergone by the periodic orbits [1–3]. Adding new, properly chosen, terms in the original Hamiltonian breaks these symmetries and forces the bifurcation patterns to unfold into the generic classification of Meyer [4]. A previous study of the unfolding of the isochronous bifurcation subjected to a single reflexion symmetry was presented by Ozorio de Almeida and de Aguiar [5].

Other important work concerning the bifurcation of periodic orbits in the presence of discrete symmetries has been developed by W. Schweizer [6], Mao and Delos [7], and Meyer *et al.* [8] for the problem of an atom placed in a uniform magnetic field. In that case the symmetries under consideration are different from those treated by this paper, and the bifurcation patterns obtained are also distinct.

In Ref. [8] an analytical study of generic two-parameter bifurcations is presented for the so-called “isochronous” (same period) and periodic doubling bifurcations.

A nice and very complete review of experimental versus theoretical results for the hydrogen atom near the ionization threshold in terms of periodic orbits and their bifurcations is presented in Ref. [9].

In this paper we study numerically the breakdown of both  $(t \rightarrow -t)$  and  $(x \rightarrow -x)$  symmetries in terms of Poincaré sections and periodic orbits, showing the local unfolding of the bifurcation patterns and the global re-arranging of the periodic families for two selected bifurcations. The Hamiltonian chosen for our numerical studies describes a charged particle of unity mass moving on a two-dimensional surface and subjected to a constant magnetic field  $B_0$  perpendicular to this surface,

$$\mathcal{H}(x, y, p_x, p_y) = \frac{1}{2}(p_x + \beta y)^2 + \frac{1}{2}(p_y - \beta x)^2 + V(x, y), \quad (1.a)$$

where  $\beta = eB_0/2c$ ,  $e$  is the electric charge, and  $c$  is the velocity of light.

The potential  $V(x, y)$  was chosen as

$$V(x, y) = \left( y - \frac{x^2}{2} + \gamma x^3 \right)^2 + \mu \frac{x^2}{2}; \quad \mu = 0.1 \quad (1.b)$$

and reduces to the well studied Nelson potential [10] when  $\gamma = 0$ .

Therefore, with  $\beta = \gamma = 0$ , Eq. (1) represents a non-generic but well-known system. Switching on  $\beta$  and  $\gamma$  breaks the time-reversal and  $x$ -reflexion symmetries, respectively. The aim of this paper is to study some aspects of this “non-generic to generic” transition considering small values of  $\beta$  and  $\gamma$ .

The paper is organized as follows: in Section 2 we discuss the symmetries of the Hamiltonian system (1) as a function of  $\beta$  and  $\gamma$ . In Section 3 we study the effects of  $\gamma$  and  $\beta$  in the Poincaré sections, switching the parameters one at a time. In Section 4 we concentrate on the periodic orbits and make a careful analysis of some bifurcation patterns as a function of  $\beta$  and  $\gamma$ . The symmetry breaking is also shown in terms of  $E \times \tau$  (energy  $\times$  period) plots where the split of degenerate families is observed. Finally, in Section 5, we make some concluding remarks.

## II. SYMMETRIES AND PERIODIC ORBITS

In what follows we shall introduce the notation  $\mathcal{H}_{\beta\gamma}$  to describe the full Hamiltonian (1). The symbol  $\mathcal{H}_{\beta 0}$ , for instance, represents the case where  $\gamma = 0$  and  $\beta \neq 0$ . Let us first consider the most symmetric case  $\mathcal{H}_{00}$  (where  $\beta = \gamma = 0$ ). Defining the four-vector

$$z = \begin{pmatrix} x \\ y \\ p_x \\ p_y \end{pmatrix}$$

we note that, in this case, the Hamiltonian (1) is invariant under

$$R_1 = \begin{pmatrix} 1 & 0 & 0 & 0 \\ 0 & 1 & 0 & 0 \\ 0 & 0 & -1 & 0 \\ 0 & 0 & 0 & -1 \end{pmatrix} \quad (2)$$

and

$$R_2 = \begin{pmatrix} -1 & 0 & 0 & 0 \\ 0 & 1 & 0 & 0 \\ 0 & 0 & -1 & 0 \\ 0 & 0 & 0 & 1 \end{pmatrix} \quad (3)$$

(corresponding to time-reversal and  $x$ -reflexion, respectively) in the sense that

$$\mathcal{H}(R_1 z) = \mathcal{H}(R_2 z) = \mathcal{H}(z).$$

Although  $R_1$  and  $R_2$  look very much alike, they have different natures, as can be seen in terms of the Hamiltonian's equations of motion,

$$\dot{z} = J \nabla_z \mathcal{H},$$

where  $J$  is the usual symplectic matrix

$$J = \begin{pmatrix} 0 & 0 & 1 & 0 \\ 0 & 0 & 0 & 1 \\ -1 & 0 & 0 & 0 \\ 0 & -1 & 0 & 0 \end{pmatrix}$$

and

$$\nabla_z = \begin{pmatrix} \partial/\partial x \\ \partial/\partial y \\ \partial/\partial p_x \\ \partial/\partial p_y \end{pmatrix}.$$

Applying  $R_i$  to both sides yields

$$(R_i \dot{z}) = R_i J \nabla_z H(z).$$

Defining  $w = R_i z$  and using

$$JR_1 = -R_1 J$$

$$JR_2 = R_2 J,$$



It is important to understand the degeneracies in the periodic orbit families. If  $z(t)$  is a symmetric rotation of  $\mathcal{H}_{00}$ , for instance, then  $R_1 z(t)$  is another symmetric rotation that corresponds to the former orbit traversed in the opposite direction (since  $R_2 z(t) = z(t)$  it does not represent a new orbit). This fact accounts for the twofold degeneracy in the table above. A similar reasoning applies to the other cases.

The periodic orbits of  $\mathcal{H}_{0\gamma}$ , on the other hand, may be only asymmetric rotations or librations and those of  $\mathcal{H}_{\beta 0}$  may be symmetric or asymmetric rotations. The periodic orbits of  $\mathcal{H}_{\beta\gamma}$  are always asymmetric rotations.

Most of the simple periodic orbits of the  $\mathcal{H}_{00}$  (the Nelson Hamiltonian) were found and studied by Baranger and Davies [10] and are displayed in Fig. 1. Since the potential is harmonic along the invariant plane defined by  $x = p_x = 0$ , this plane is foliated by a family of "vertical" ( $y$ -direction) oscillations of constant period  $\tau = 2\pi/\sqrt{2}$ , named  $V$  in Fig. 1.

In the energy range  $(0.0, 0.300)$ , the vertical family presents three main bifurcations:

1. period quadruplication ( $E \approx 0.019$ ), generating two new families: the stable family  $A$  and the unstable family  $H$ , both symmetric librations.
2. period triplication ( $E \approx 0.077$ ) generating two new degenerate families, the stable family  $C$  (symmetric rotation) and the unstable family  $P$  (asymmetric libration).
3. period duplication at ( $E \approx 0.136$ ) generating the stable family  $B$  (symmetric libration). At this point the vertical family goes unstable.

Another important family is the horizontal family  $H$ . In the energy range  $(0, 0.300)$ , the horizontal family  $H$  presents two isochronous bifurcations (bifurcations without period change [1, 2]) generating one stable family of symmetric rotations and one unstable family of asymmetric librations. This bifurcation point is indicated in Fig. 1 by a symbol  $4^2$  near  $\tau \approx 21$ .

In what follows we shall change the names of some periodic families to make the identification of their genesis easier. The families originating at the quadruplication of the vertical family,  $A$  and  $H$  will be called  $V4S_{00}$  and  $V4U_{00}$ , respectively, where  $V$  stands for the "mother" orbit, 4 for quadruplication,  $S$  or  $U$  for stable or unstable and the subscript "00" for  $\gamma = \beta = 0$ . Analogously,  $C$  and  $P$  will be renamed  $V3S_{00}$  and  $V3U_{00}$  and the orbit  $B$  (see Fig. 1) will become  $V2_{00}$ . The families originating at the isochronous bifurcation of the horizontal family  $H_{00}$ , will be called  $R_{00}$  and  $L_{00}$ , where  $R$  and  $L$  denote rotations and librations, respectively. (Since these are the only important bifurcations of  $H_{00}$ , we shall not use the notation  $H1S_{00}$  and  $H1U_{00}$  in this case). Note that  $H_{00} = V4U_{00}$ . If the subscripts are omitted, like in  $V3S$ , for example, we shall be referring generically to the triplication of the vertical family.

### III. POINCARÉ SECTIONS

It can be checked easily that the energy surfaces of  $\mathcal{H}_{\beta\gamma}$  are compact for all values of  $\gamma$  and  $\beta$ . Therefore, most trajectories will be recurrent and the Poincaré sections

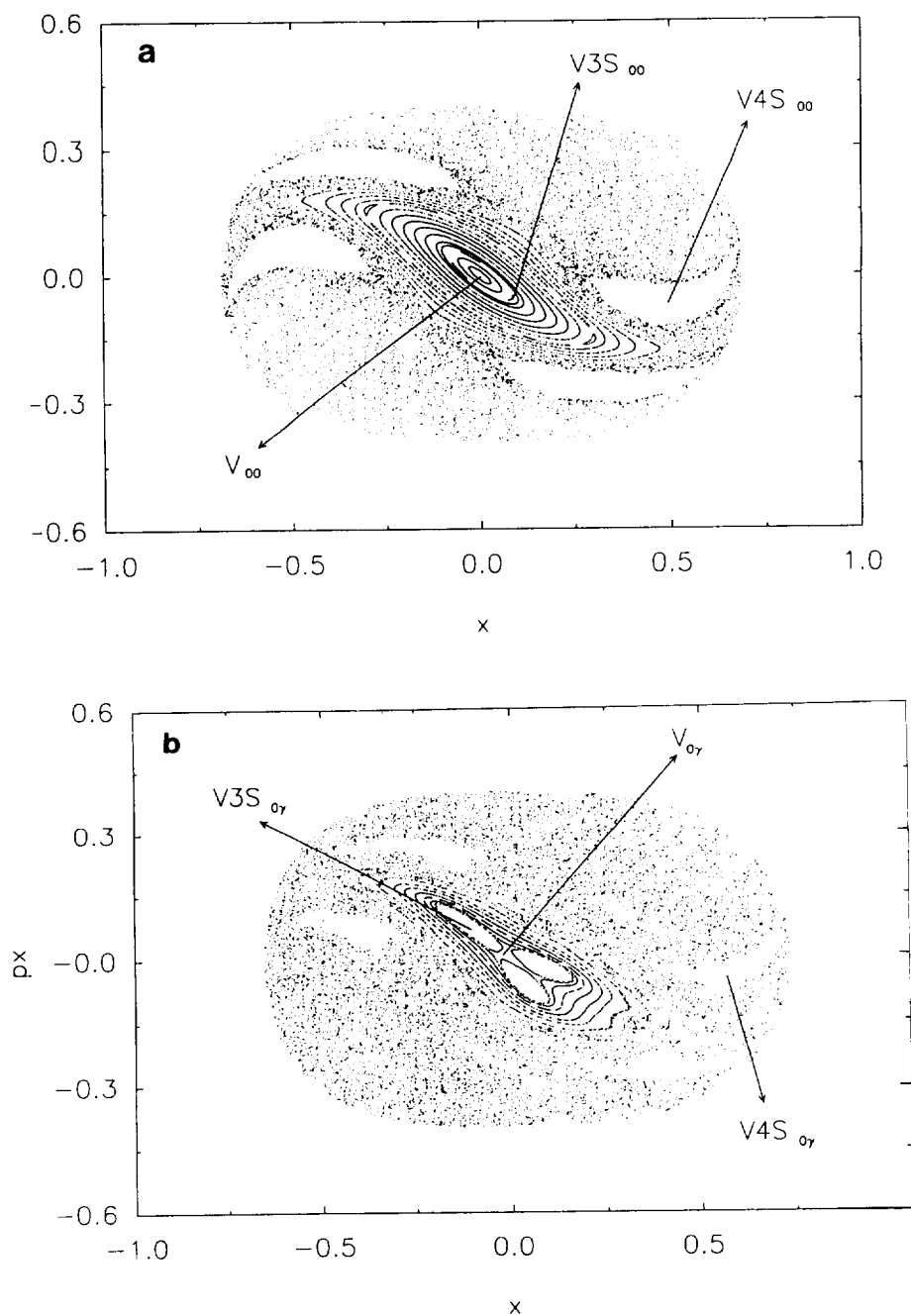


FIG. 2.  $x-p_x$  Poincaré sections at energy  $E=0.08$  for: (a)  $\mathcal{H}_{00}$ ; (b)  $\mathcal{H}_{0\gamma}$  with  $\gamma=0.1$ ; (c)  $\mathcal{H}_{\beta\gamma}$  with  $\gamma=0.1$  and  $\beta=0.03$ .

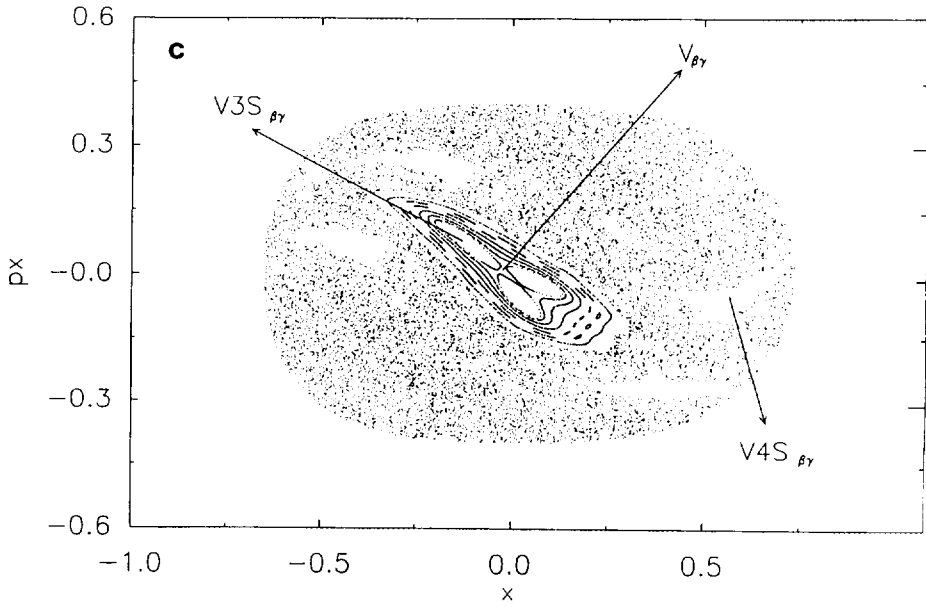


FIG. 2 — Continued

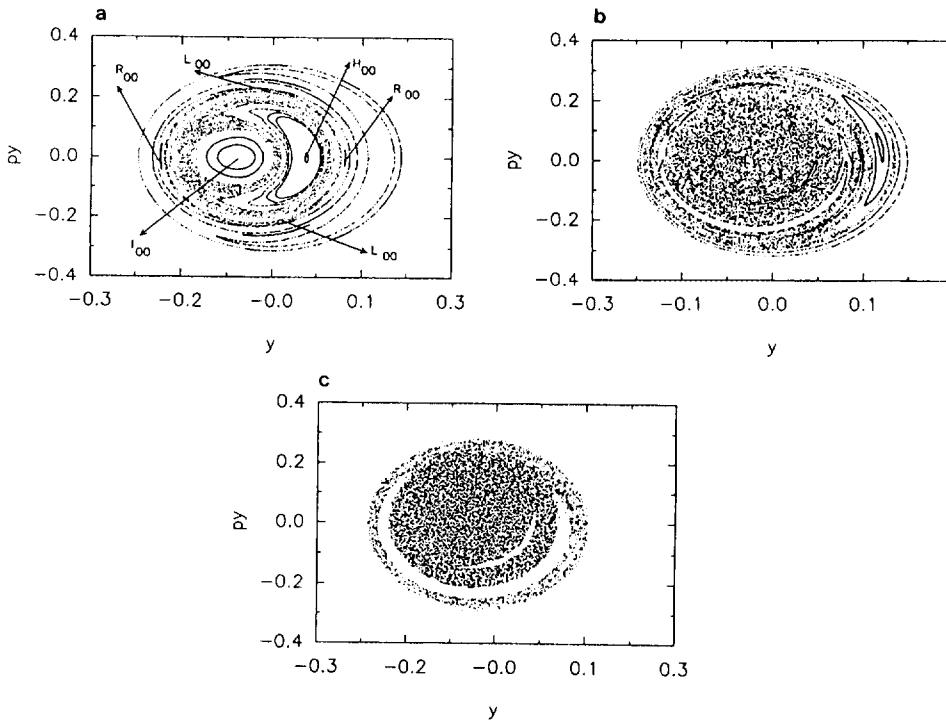


FIG. 3.  $y-p_y$  Poincaré sections at energy  $E=0.05$  for: (a)  $\mathcal{H}_{00}$ ; (b)  $\mathcal{H}_{0\gamma}$  with  $\gamma=0.1$ ; (c)  $\mathcal{H}_{\beta\gamma}$  with  $\gamma=0.1$  and  $\beta=0.03$ .

can be used to extract qualitative information about the phase space structure. In this section we shall present  $x-p_x$  and  $y-p_y$  Poincaré sections of the Hamiltonian given by Eq. (1) for three different situations. Figure 2 shows the  $x-p_x$  sections of  $\mathcal{H}_{00}$ ,  $\mathcal{H}_{0\gamma}$  with  $\gamma=0.1$  and  $\mathcal{H}_{\beta\gamma}$  with  $\gamma=0.1$  and  $\beta=0.03$  at energy  $E=0.08$ . In all cases the orbits  $V$ ,  $V3S$ , and  $V4S$  can be easily identified. The size of the chaotic regions observed in these sections are about the same. The only qualitative change appears to be shape of islands around  $V3S$ .

The  $y-p_y$  Poincaré sections corresponding to the same situations of Fig. 2 are presented in Fig. 3 at  $E=0.05$ . It is now clear that the effect of the symmetry breaking terms have introduced large instabilities in the phase space. This sort of instabilities have also been reported by Guckenheimer and Mahalov [14] in a different context.

We observe in Fig. (3a) the principal branches of the horizontal family  $H_{00}$ , the rotations  $R_{00}$  and the librations  $L_{00}$ . We also observe the stable branch of family  $I$ , renamed  $I_{00}$  (see Fig. 1). Its unstable branch gives rise to a chaotic region in the center of the section. In Fig. (3b), where  $\gamma=0.1$  we observe a more chaotic behaviour and some new bifurcations. In Fig. (3c), where  $\gamma=0.1$  and  $\beta=0.03$  the behaviour is more chaotic still.

#### IV. EFFECTS ON THE PERIODIC ORBITS

Periodic orbits play a very important role in the theory of dynamical systems. Moreover, it has been shown by Gutzwiller [15], that the periodic orbits are the fundamental ingredient in the semiclassical connection between classical and quantum mechanics. As can be seen by comparing Figs. 1, 2a, and 3a (for  $\mathcal{H}_{00}$ ), the knowledge of the  $E \times \tau$  (energy versus period) plots for the families of periodic orbits is complementary to the Poincaré sections. From the later we can readily measure the size of the chaotic regions, but we could hardly locate the individual orbits. From the  $E \times \tau$  plots, on the other hand, it is impossible to predict the global behaviour of a section. Besides, a Poincaré section gives information at constant energy, while  $E \times \tau$  plots shows the behaviour "across" the energy surface.

The periodic solutions of generic Hamiltonian systems form one-parameter families (the parameter may be the energy  $E$  or the period  $\tau$ ). When this parameter is changed, we move along the family and there exist values at which new families are generated. The points where this happens are called bifurcation points. The period of the bifurcated trajectories,  $\tau_b$ , will be integer multiples of the period of the original trajectory,  $\tau_0$ , at the bifurcation point:

$$\tau_b = n\tau_0. \quad (6)$$

An extensive numerical analysis of the periodic solutions and bifurcations of Hamiltonian systems with two-degrees of freedom can be found in Refs. [1, 10]. A complete classification of the bifurcations of periodic orbits in Hamiltonian systems with time-reversal and  $x$ -reflexion symmetry can be found in Refs. [1, 2].



The monodromy matrix  $\mathbf{M}$  contains the information about the stability of a periodic trajectory. It describes how a small perturbation away from the orbit changes after one period. For two-degrees of freedom  $\mathbf{M}$  is a  $4 \times 4$  matrix. Two of its eigenvalues are always unity, and the other two have unity product. Therefore they are either complex conjugates ( $e^{i\alpha}$ ,  $e^{-i\alpha}$ ) or real inverses ( $\pm e^{+\mu}$ ,  $\pm e^{-\mu}$ ). In the first case, the trajectory is stable and the trace of  $\mathbf{M}$  ( $\text{tr } M$ ) is between zero and four. In the second case, the trajectory is unstable and the  $\text{tr } M$  is either less than zero or greater than four.

In isochronous ramifications, where the matrix  $\mathbf{M}$  has four unity eigenvalues,  $\text{tr } M = 4$ . At a period doubling two eigenvalues are  $(-1)$  and consequently  $\text{tr } M = 0$ . There also occurs period triplication where  $\text{tr } M = 1$ , period quadruplication where  $\text{tr } M = 2$ , and so on. In summary, the value of  $\text{tr } M$  determines the stability and bifurcation points of the periodic orbit family.

In this paper we shall concentrate in the study of only two selected bifurcations. The first is the sequence of two very close isochronous bifurcations undergone by the horizontal family  $H_{00}$ . The second situation is the periodic triplication of the vertical family  $V_{00}$ . In both cases the bifurcations appearing in  $\mathcal{H}_{00}$  are non-generic and must unfold into the generic cases as  $\gamma$  and  $\beta$  are turned on.

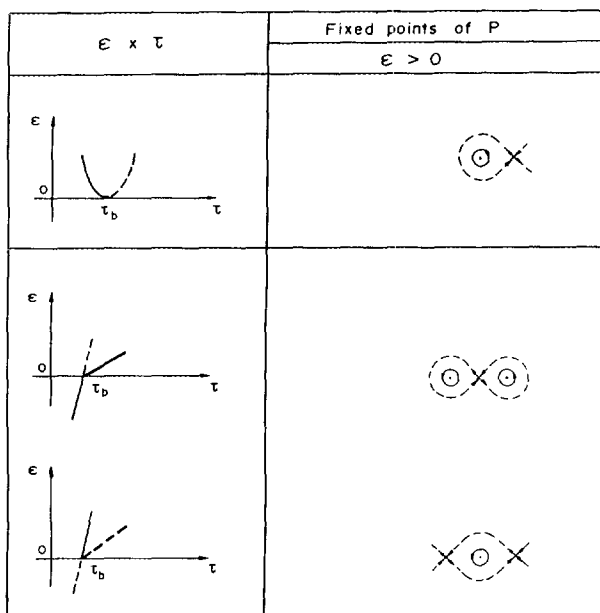


FIG. 4. Schematic  $E \times \tau$  plot and Poincaré section for the possible isochronous bifurcations of  $\mathcal{H}_{00}$ . The full(dashed) line indicates stable(unstable) orbits. Thick lines (full or dashed) indicate degenerate families. The upper part indicates the generic bifurcation, whereas the lower part shows the pitchfork and inverse-pitchfork non-generic possibilities.

Figure 4 shows schematically the  $E \times \tau$  plots and the Poincaré sections for the possible kinds of isochronous bifurcations depending on the symmetries of the Hamiltonian. The generic situation corresponds to a saddle-center bifurcation where no new family is generated: the original family only switches from stable to unstable. In the presence of one or two discrete symmetries it may happen that a pair of (degenerate) families is created through a pitchfork bifurcation. It is important to note that this sort of non-generic bifurcation always occurs at the expense of a symmetry loss: the bifurcated pair has always one symmetry less than the original family.

Figure 5 shows the possibilities for period tripling. In the symmetric case,  $\mathcal{H}_{00}$ , two new families of orbits (each twofold degenerate) are created by losing a different symmetry each: a pair of rotations and a pair of librations are generated. If the system has only one or no symmetries at all, only the generic case occurs: a single unstable new family exists both above and below the bifurcation point, where it coalesces with the original family.

Let us first consider the isochronous bifurcation. Figures 6 and 7 display a blowup of the  $E \times \tau$  plot for the horizontal family of  $\mathcal{H}_{00}$  near the bifurcation point. Figure 8 shows the  $x-y$  projections of the orbits involved in this bifurcation at three different energies to illustrate the evolution of these orbits along their families.

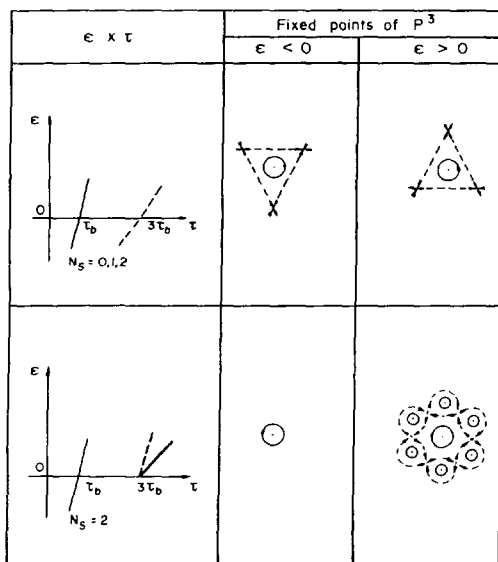


FIG. 5. Schematic  $E \times \tau$  plot and Poincaré section for the possible period tripling bifurcations of  $\mathcal{H}_{00}$ . See caption Fig. 4 for notation. The upper part indicates the generic bifurcation, whereas the lower part shows the bifurcation when both symmetries are present.

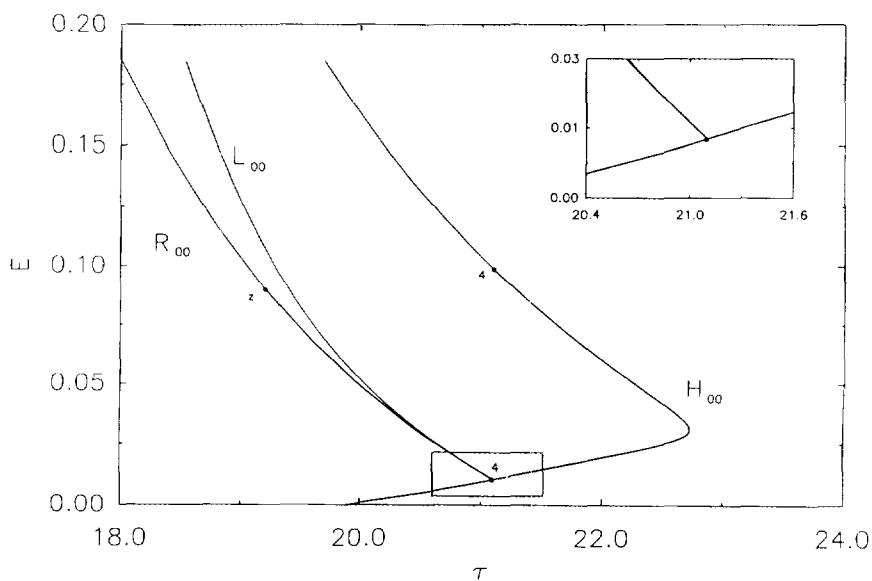


FIG. 6.  $E \times \tau$  plot of the Horizontal family of  $\mathcal{H}_{00}$ . See caption of Fig. 1 for notation.

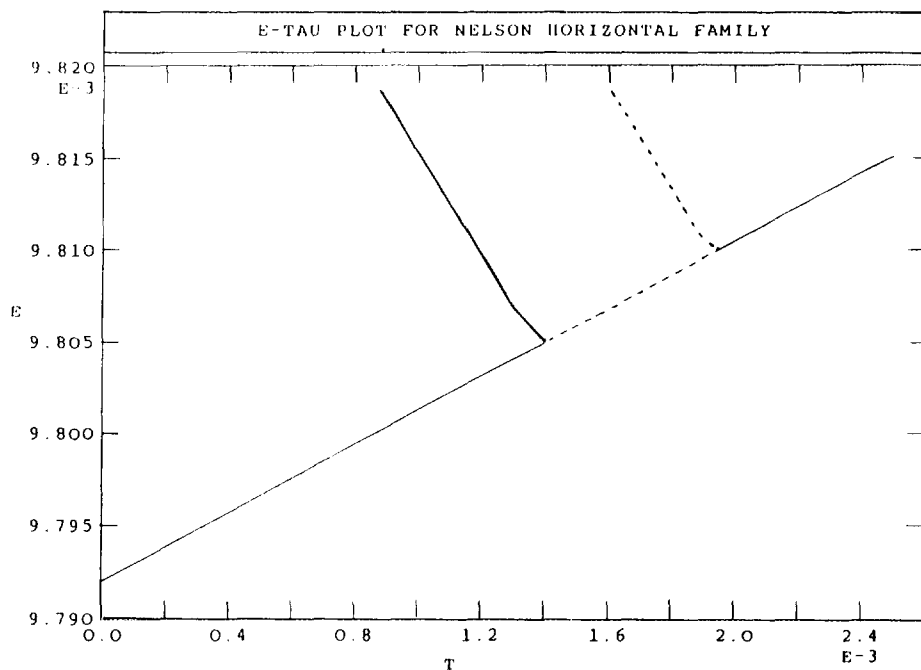


FIG. 7. Blow up of Fig. 6 showing the two consecutive isochronous bifurcations occurring of  $H_{00}$ . See caption of Fig. 4 for notation.

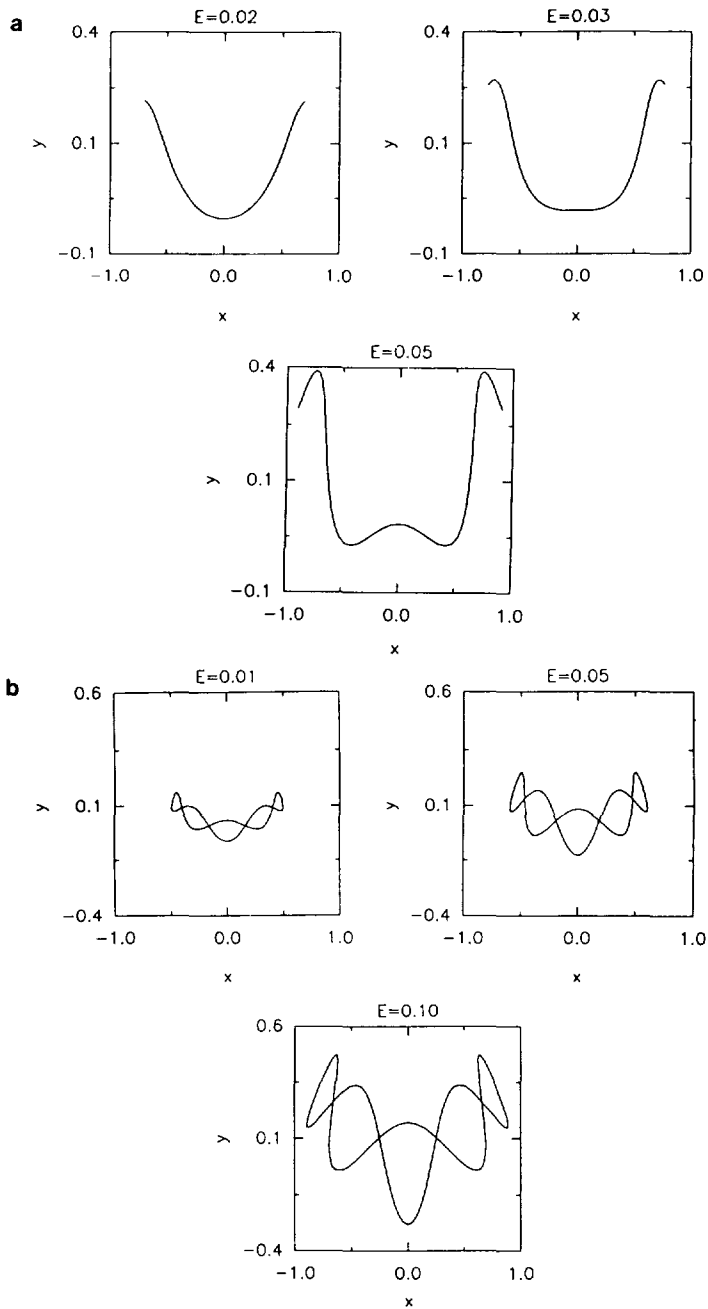
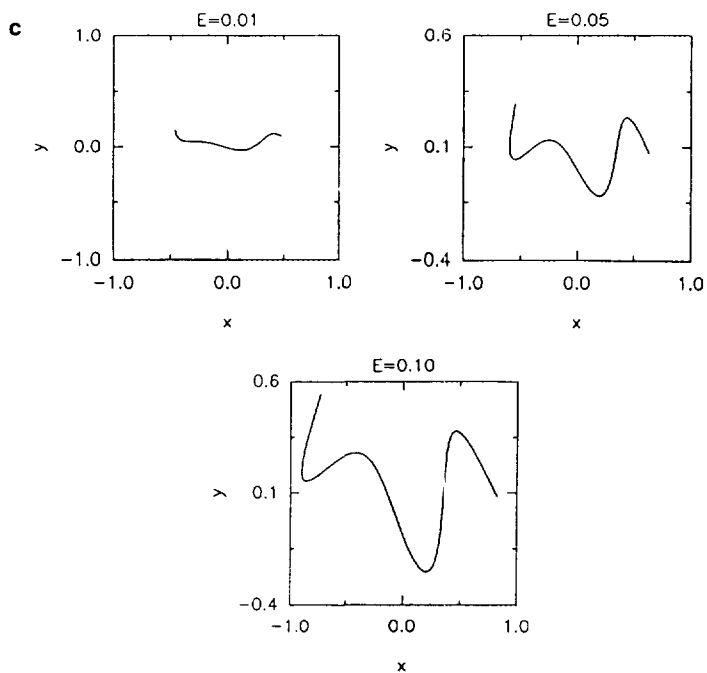
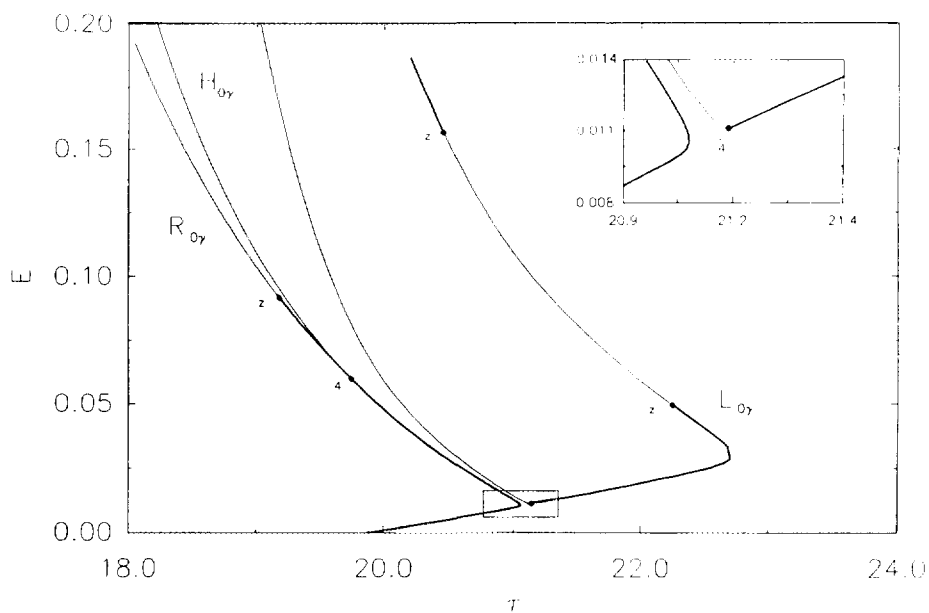


FIG. 8. Projections onto the  $x-y$  plane of the periodic orbits involved in the isochronous bifurcations of  $H_{00}$ : (a) shows the symmetric librations  $H_{00}$ ; (b) shows the symmetric rotations  $R_{00}$ ; (c) shows the asymmetric librations  $L_{00}$ . All orbits are shown at three different energies as indicated in the figures.

FIG. 8 — *Continued*FIG. 9.  $E \times \tau$  plot of the horizontal family of  $\mathcal{H}_{\gamma,0}$  for  $\gamma=0.1$  (compare with Fig. 6).

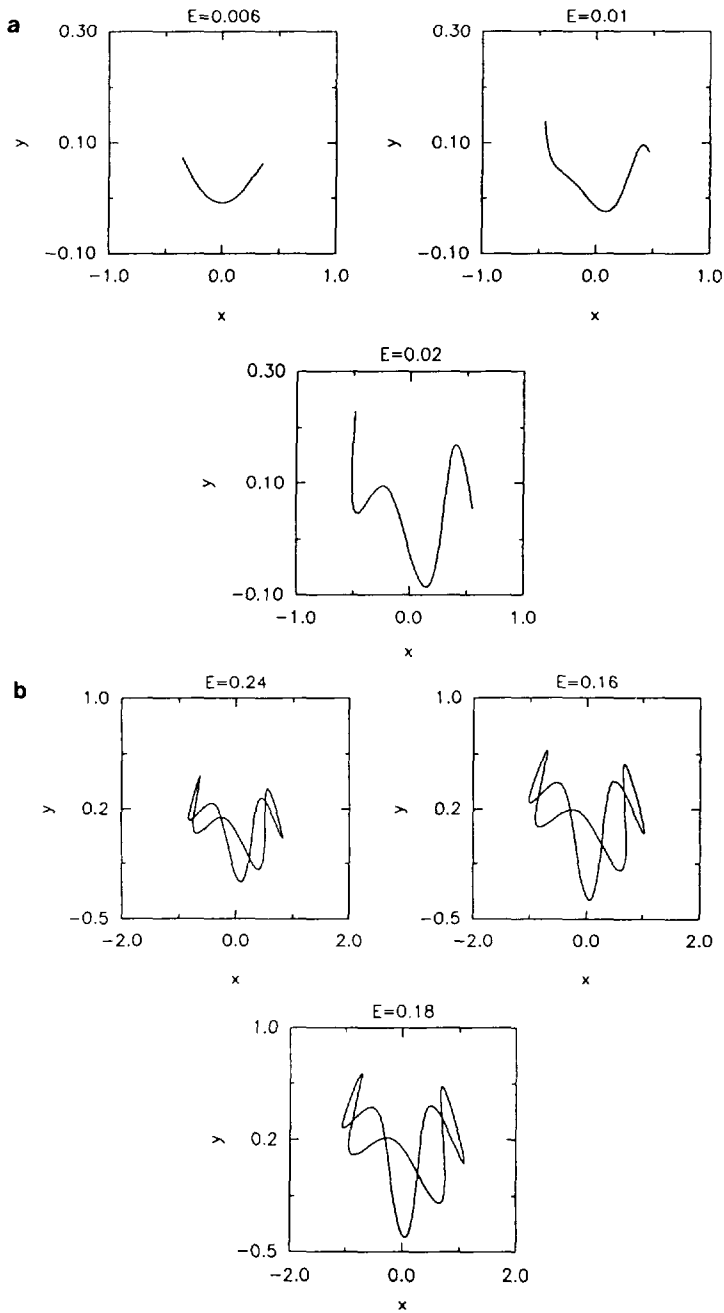
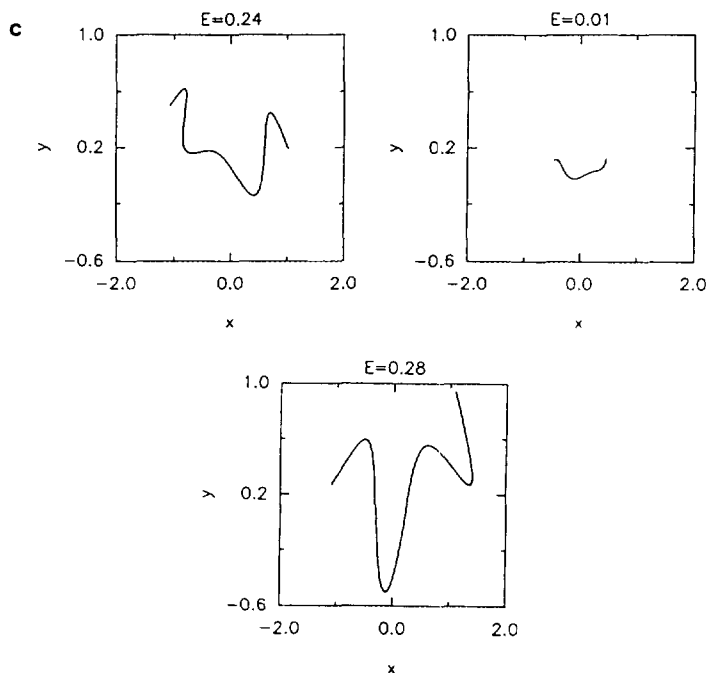


FIG. 10. Projections onto the  $x-y$  plane of the periodic orbits involved in the isochronous bifurcations of  $H_{0\gamma}$  for  $\gamma = 0.1$ : (a) shows the asymmetric librations  $H_{0\gamma}$ ; (b) shows the asymmetric rotations  $R_{0\gamma}$ ; (c) the asymmetric librations  $L_{0\gamma}$ . All orbits are shown at three different energies as indicated in the figures.

FIG. 10—*Continued*

When the parameter  $\gamma$  is turned on, the isochronous bifurcation where the  $x$ -symmetry would be lost (generating the librations  $L_{00}$ ) cannot occur, since that symmetry does not exist. The net effect is shown in Fig. 9: the old family of librations detach from the horizontal family, producing a generic isochronous situation while the horizontal family continues to be stable [5, 8]. Figure 10 shows the  $x-y$  projections of the periodic orbits (compare with Fig. 8). The bifurcation of  $H_{00}$ , where the time-reversal symmetry was lost continues to exist non-generically for  $H_{0\gamma}$ . This bifurcation unfolds when  $\beta$  is turned on exactly in the same way, detaching one more branch from the horizontal family. Figure 11 shows schematically this sequence of detachings, unfolding the non-generic pitchforks into saddle-centers.

Now we study the unfolding of the period tripling bifurcation. Figure 12 shows the  $E \times \tau$  plot of the non-generic bifurcation undergone by the  $V_{00}$  family of  $\mathcal{H}_{00}$ , which corresponds to the second type show in Fig. 5. Figure 13 shows the  $x-y$  projections of the orbits involved. When  $\gamma$  is turned on, two effects appear at same time: first the bifurcation point  $P$ , which was at the point of minimum energy reached by the bifurcated orbits  $V3S$  and  $V3U$  (see Fig. 12), is shifted upwards as shown in the detail of Fig. 14. This effect unfolds the period tripling. Second, the lower branch of the tripled orbits very quickly becomes stable through a generic isochronous bifurcation and then becomes unstable again via a non-generic pitchfork-like isochronous branching. Figure 15 shows the  $x-y$  projections of the

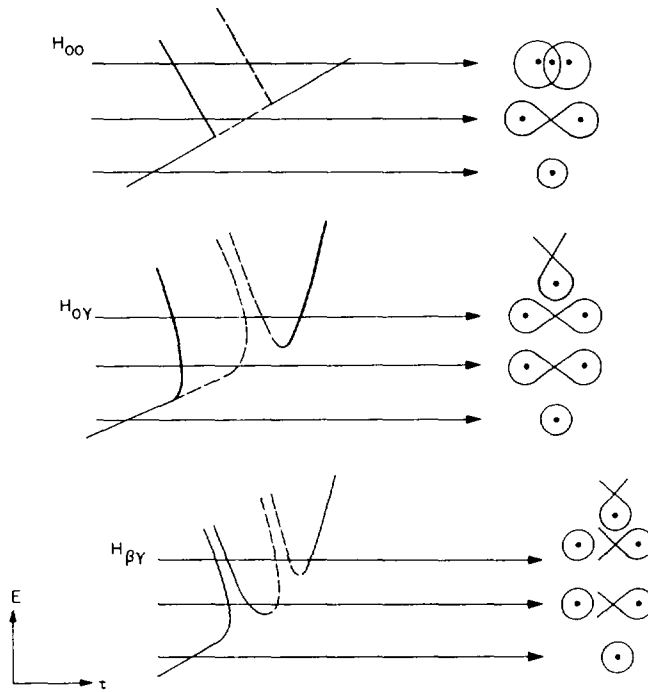


FIG. 11. Schematic  $E \times \tau$  plots and Poincaré sections showing the breakdown of symmetries at the isochronous bifurcations of Horizontal family. The system is (a)  $\mathcal{H}_{00}$ ; (b)  $\mathcal{H}_{\gamma 0}$ ; (c)  $\mathcal{H}_{\beta \gamma}$ . See caption of Fig. 4 for notation.

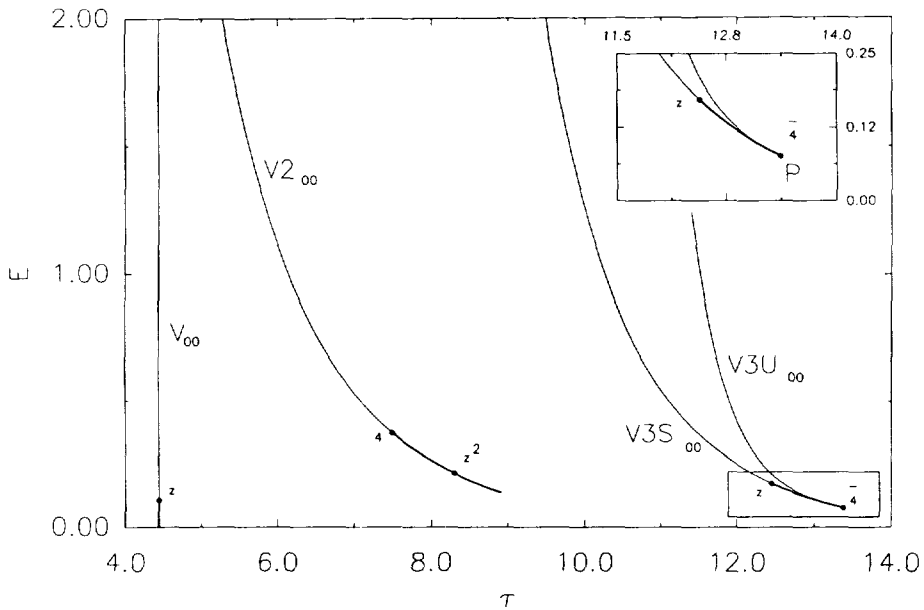


FIG. 12.  $E \times \tau$  plot of the vertical family of  $\mathcal{H}_{00}$ . See caption of Fig. 1 for notation.



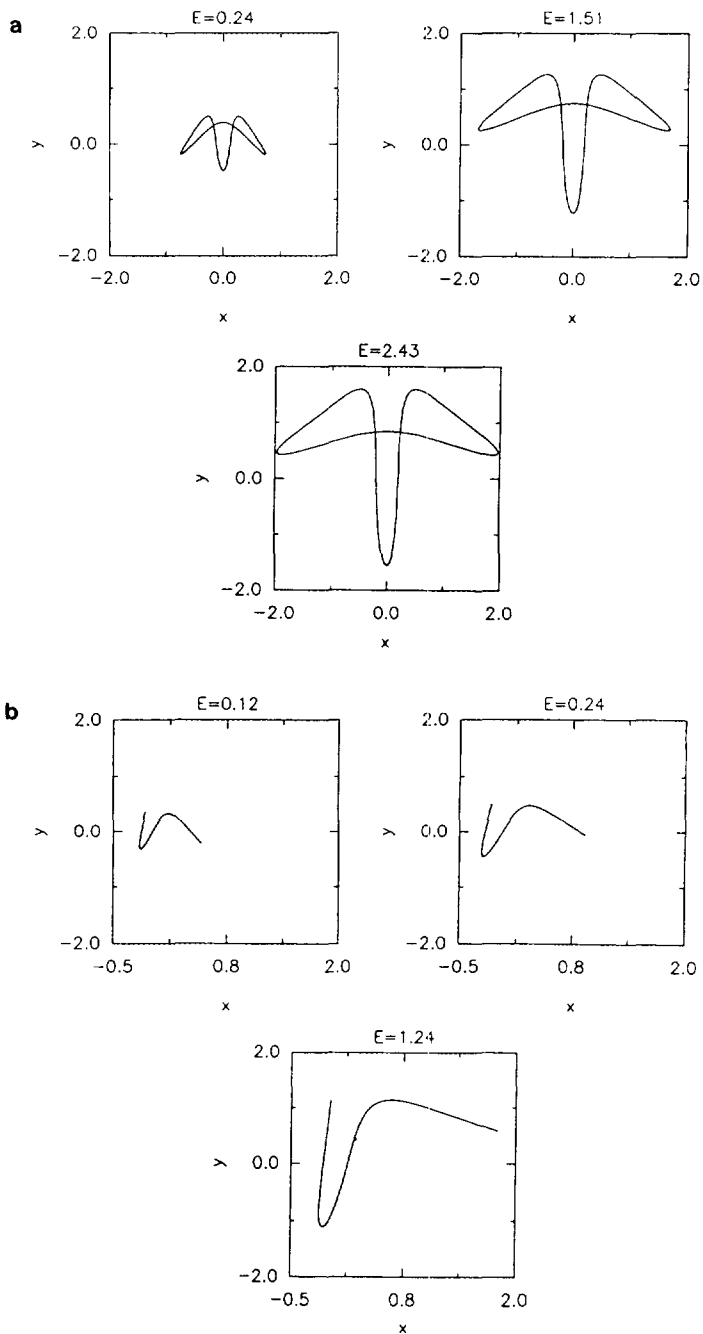


FIG. 13. Projections onto the  $x-y$  plane of the periodic orbits involved in the period tripling of the vertical family of  $\mathcal{H}_{00}$ : (a) shows the symmetric rotations  $V3S_{00}$ ; (b) shows the asymmetric librations  $V3U_{00}$ .

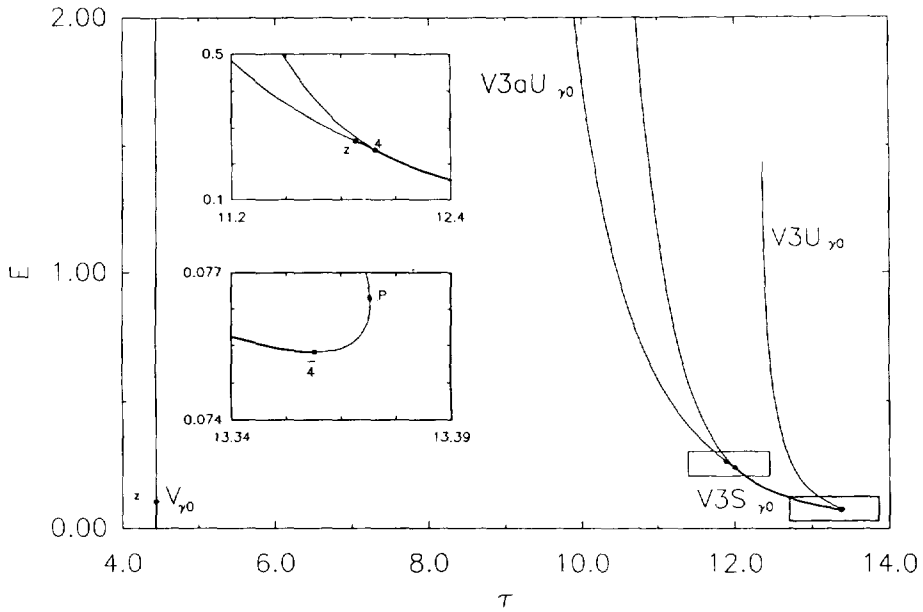


FIG. 14.  $E \times \tau$  plot of the vertical family of  $\mathcal{H}_{\gamma 0}$  for  $\gamma = 0.1$ . See caption of Fig. 1 for notation.

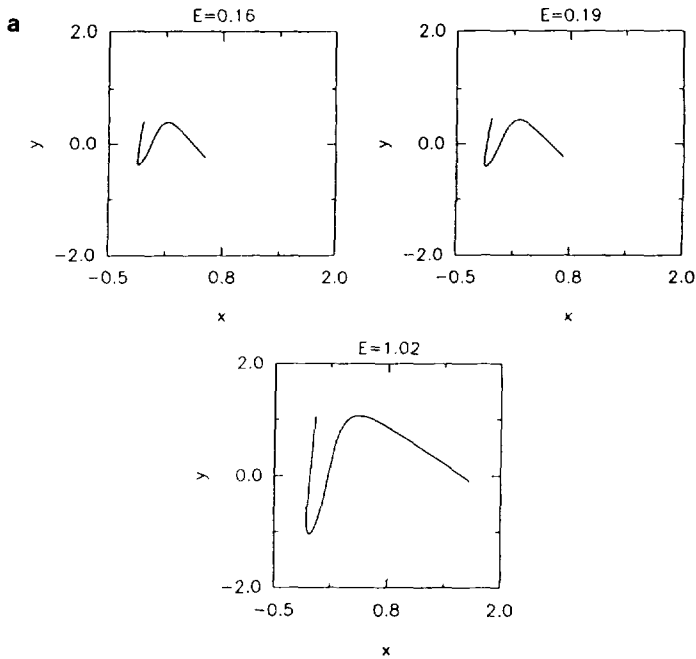


FIG. 15. Projections onto the  $x-y$  plane of the periodic orbits involved in the period tripling of the vertical family of  $\mathcal{H}_{\gamma 0}$  for  $\gamma = 0.1$ : (a) shows the asymmetric librations  $V3U_{\gamma 0}$ ; (b) shows the asymmetric librations  $V3S_{\gamma 0}$ ; (c) shows the asymmetric rotations  $V3aU_{\gamma 0}$ .

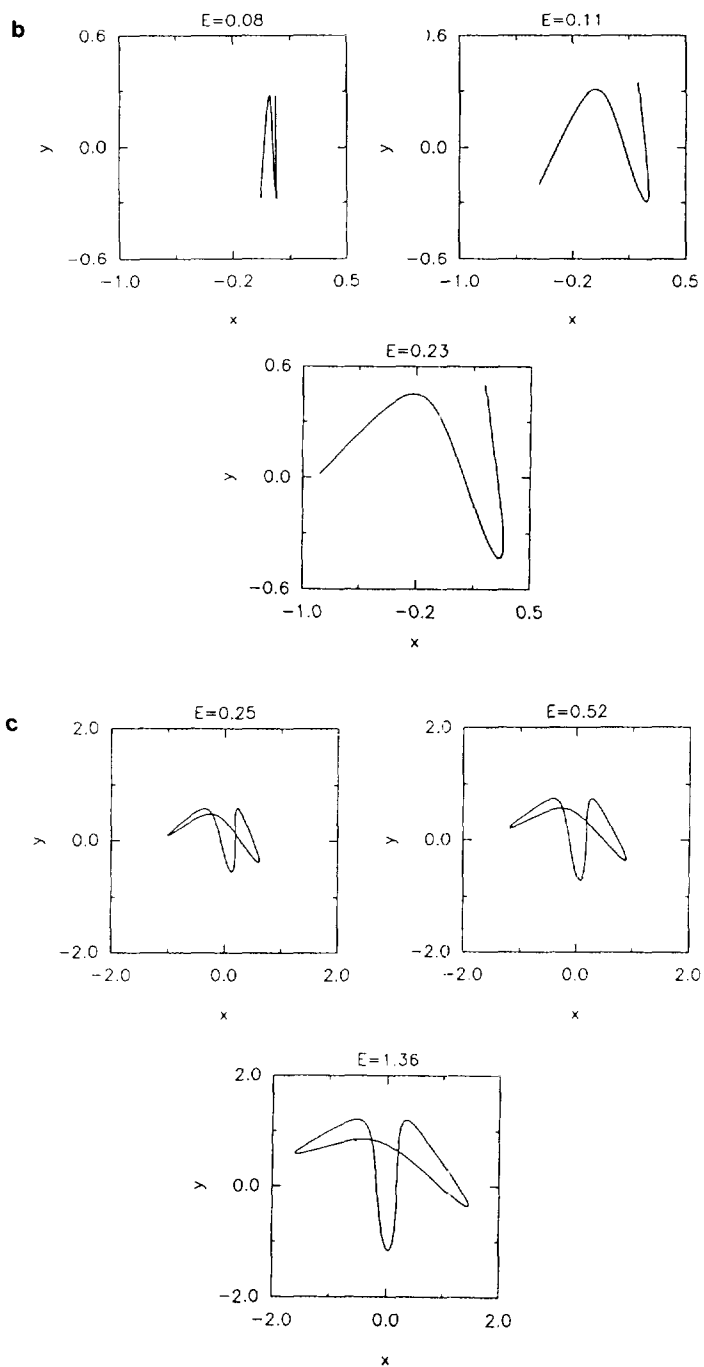


FIG. 15—Continued

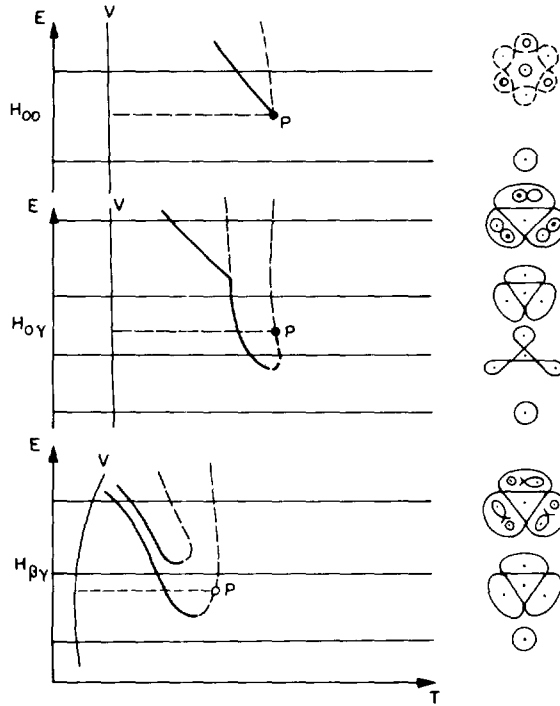


FIG. 16. Schematic  $E \times \tau$  plots and Poincaré sections showing the breakdown of symmetries at the period tripling bifurcation of the vertical family. The system is (a)  $\mathcal{H}_{00}$ ; (b)  $\mathcal{H}_{\gamma 0}$ ; (c)  $\mathcal{H}_{\beta \gamma}$ . See caption of Fig. 4 for notation.

orbits (compare with Fig. 13). Again, when  $\beta$  is turned on this last non-generic bifurcation unfolds in the way discussed before. Figure 16 shows schematically the complete unfolding.

## V. CONCLUDING REMARKS

We have studied the breakdown of two reflexion symmetries in a non-integrable Hamiltonian system with two degrees of freedom. From the classical point of view we have concentrated on the unfolding of only two selected bifurcations. As we have seen, the reduction of symmetries forces the degenerate families of periodic orbits to split into separate families, changing the topology of the  $E \times \tau$  plot. Although we have not checked the unfolding of all possible bifurcations, we believe that similar effects would be observed in more complicated cases. We have also observed an increase in the phase-space volume filled with chaotic trajectories as the symmetries are broken.

It is important to point out that, while the unfolding of the pitchfork bifurcation into a saddle center plus an independent orbit is generic [5, 8], no formal results

concerning the unfolding of the periodic tripling (or any other bifurcation) is known, and a complete theory is still lacking.

Quantum mechanical effects due to symmetry reduction can also be studied. The ideal effect to be observed would be the split of the peaks in the Fourier transform of the smoothed density of states according to the split of the corresponding periodic orbit families [8, 9, 16–19]. Such a split of the horizontal family, as shown in Fig. 9, for instance, would require a resolution in the Fourier spectrum of  $\Delta\tau \approx 0.1$ . Unfortunately, for this particular Hamiltonian, this gap does not change appreciably with the parameter  $\gamma$ . Therefore, a simple estimate shows that a resolution of  $\Delta\tau \approx 0.1$  would be possible only for very small values of  $\hbar$  ( $\hbar \approx 10^{-6}$ ) which would imply the diagonalization of very large matrices. A few quantum mechanical calculations have been performed with  $\hbar = 6 \times 10^{-3}$  but no striking effects could be noted at this (poor) resolution. It should be noted, however, that experimental measurements of atomic spectra show that the symmetry breaking effects are indeed observable [9].

#### ACKNOWLEDGMENTS

It is a pleasure to thank A. M. Ozorio de Almeida, F. A. Bajay, and M. A. Andrade Neto for helpful discussions. We are also thankful to Professor J. B. Delos for pointing out Ref. [7] and for sending preprints of Refs. [8, 9]. This work was partly supported by CNPq, FINEP, and FAPESP. We acknowledge their financial support.

#### REFERENCES

1. M. A. M. DE AGUIAR, C. P. MALTA, M. BARANGER, AND K. T. R. DAVIES, *Ann. Phys. (N.Y.)* **180** (1987), 167–205.
2. M. A. M. DE AGUIAR AND C. P. MALTA, *Physica D* **30** (1988), 413.
3. R. RIMMER, *J. Differential Eqs.* **29** (1978), 329.
4. K. R. MEYER, *Trans. Amer. Math. Soc.* **149** (1970), 95.
5. M. A. M. DE AGUIAR AND A. M. OZORIO DE ALMEIDA, *Physica D* **30** (1990), 391–402.
6. W. SCHWEIZER, R. NIEMEIER, G. WUNNER, AND H. RUDER, *Z. Phys. D* **25** (1993), 95.
7. J.-M. MAO AND J. B. DELOS, *Phys. Rev. A* **45** (1992), 1746.
8. K. R. MEYER, J. B. DELOS, AND J.-M. MAO, in "Proceedings, Conservative Systems and Quantum Chaos Workshop, Fields Institute, Waterloo, Canada, 1992" (D. Rod, Ed.), to appear.
9. J. MAIN, G. WIEBUSCH, K. WELGE, J. SHAW, AND J. B. DELOS, *Phys. Rev.*, in press.
10. M. BARANGER AND K. T. R. DAVIES, *Ann. Phys.* **177** (1987), 330–358.
11. R. L. DEVANEY, *Trans. Am. Math. Soc.* **218** (1976), 89.
12. J. A. G. ROBERTS AND G. R. W. QUISP, *Phys. Rep.* **216** (1992), 63–177.
13. M. BARANGER, K. T. R. DAVIES, AND J. H. MAHONEY, *Ann. Phys. (N.Y.)* **186** (1988), 95–111.
14. J. GUCKENHEIMER AND A. MAHOLOV, *Phys. Rev. Lett.* **68** (1992), 2257.
15. M. C. GUTZWILLER, *J. Math. Phys.* **12** (1971), 343.
16. M. C. GUTZWILLER, *J. Math. Phys.* **11** (1970), 791.
17. D. WINTGEN, *Phys. Rev. Lett.* **61** (1988), 16.
18. C. P. MALTA AND A. M. OZORIO DE ALMEIDA, *J. Phys. A: Math. Gen.* **23** (1990), 4137.
19. C. P. MALTA, A. M. OZORIO DE ALMEIDA, AND M. A. M. DE AGUIAR, *Phys. Rev. A* **47** (1993), 1625.